

PRECISION CURRENT TRANSDUCTOR
FOR THE FERMILAB BOOSTER MAGNET POWER SUPPLY

J. A. Dinkel and A. R. Donaldson
Fermi National Accelerator Laboratory*
Batavia, Illinois 60510

Summary

The Fermilab Booster synchrotron requires precise injection and extraction field regulation ($\pm 0.001\%$ repeatability).¹ To achieve this tolerance with a current regulator requires that the current measuring device have a high degree of resolution, stability, and a high output level.

To meet this criteria, a transducer using the second-harmonic magnetic modulator technique was chosen. This device is capable of better than $\pm 0.001\%$ measurements from dc to 15 Hz for currents from 50 to 1200 A. Small signal (~ 100 A peak-to-peak) response is 3 dB down at 10 KHz. The conversion gain was chosen as 1 V/121.25 A to permit operational amplifier compatible signal levels at the output.

Introduction

The symmetrical nonlinear relationship between excitation current and magnetic flux density for a ferromagnetic material provides the physical basis for the magnetic modulator. In the second harmonic magnetic modulator a ferromagnetic core is subjected to a symmetrical ac excitation. In the absence of polarization, the magnetic flux is symmetrical and contains no even harmonics. Direct-current excitation upsets the symmetry of the B-H loop and introduces even harmonics into the spectrum of the flux waveform. The magnitude and phase of these harmonics are indicative of the magnitude and sign of the dc excitation.

In a transducer, direct current in the primary winding produces a dc flux in the ferromagnetic cores within the transducer. The second harmonic component is extracted from the spectrum and compared with a reference signal from the ac excitation source in a phase sensitive detector. The resulting dc voltage is amplified to provide a bucking current in a multturn feedback winding which cancels the primary induced dc flux in the cores. In this design, the magnetic modulator serves as a null device (flux detector) so we need not be concerned with its linearity or dynamic range.

Measuring Head

The measuring head shown in Fig. 1 contains a coupled core assembly (C_1 to C_4) to detect dc flux imbalances, and an outer core, C_5 , to decouple this assembly from the sources of dc excitation. The 2,425 turn feedback winding is wound directly over the detector assembly and decoupling core. The turns are distributed evenly around the circumference of

the toroidal assembly to reduce localized flux variations in the detector cores. These variations can occur even though

$$\frac{1}{2\pi} \int_0^{2\pi} NI \, d\theta = 0.$$

The primary winding, a single coaxial turn enclosing the flux detector and feedback winding completes the transducer measuring head.

Two pairs of cores are excited in the balanced configuration shown in Fig. 2(a). Even harmonics are generated through biasing the symmetrical magnetic properties of cores C_1 and C_2 with a dc flux. To achieve an effective measuring head design, the following criteria are considered to be essential:

1. A reasonably high impedance level must be provided for ac imbalance currents to establish good detector sensitivity.
2. All nonlinear impedances must be symmetrical with no dc excitation present (no hysteresis effects).
3. Sources of dc excitation must be effectively decoupled from the flux detector.
4. A symmetrical ac excitation signal is required.

To meet the first two criteria, cores C_3 and C_4 are added. These cores are excited from a quasi-voltage source to eliminate remnant field effects. The equivalent circuit seen by even harmonic voltages in the measuring head is shown in Fig. 2(b). An approximate impedance level at N_1 referred to the excitation winding (N_4) is:

$$Z = R_4 \left(\frac{N_1}{N_4} \right)^2, \quad (1)$$

where R_4 is chosen to overcome the magnetization current in cores C_3 and C_4 which has been measured at 3 amp turns at 3,675 Hz.

To effectively decouple the sources of dc excitation, the four detector cores are tightly coupled by winding N_3 . The impedance of the dc excitation winding N_2 is increased by the addition of C_5 . The windings are designed such that:

$$R_3 + jX_{L3} << \left(\frac{N_3}{N_1} \right)^2 \left[R_L + R_2 + j(X_{L2} + X_{LC5}) \right], \quad (2)$$

where $R_L + R_2$ represent the resistances in the dc excitation source and $X_{L2} + X_{LC5}$ represent the reactance in the dc excitation source.

* Operated by Universities Research Association Inc. under contract with the United States Energy Research and Development Administration.

$$E = K \cos \theta, \quad (4)$$

The detector cores in this device consist of 20 wraps of 1 mil Permalloy tape wound on a stainless steel bobbin 11.1 cm in diameter. Their magnetic cross section is 0.81×10^{-6} meters². The decoupling core, C_5 , is made of 2 mil silicon steel with a 5.3×10^{-5} meters² cross section. The shorted turn N_3 is 100 turns of 0.005×0.25 inch copper foil which is solder tinned after winding.

Experience has shown that feeding the coaxial primary winding at each quadrant with a slotted current divider provides a sufficiently uniform current sheet around the detector cores to produce high quality measurements (see Fig. 3).

AC Excitation

The ac excitation circuit provides a stable frequency from a low impedance source for the flux detector. A low impedance is required to provide sufficient excitation current to generate some measurable ac flux change in the detector cores with the large dc imbalance which would occur if this power were interrupted with full primary current present. The waveform is a highly symmetrical square wave at a frequency of 3,675 Hz. The frequency selection is based on a compromise between core losses on one hand and signal-to-noise ratio and frequency response on the other. The frequency thus chosen lies in the optimum range and permits the use of a commercially available telemetry filter for extraction of the second harmonic.

The excitation source is an integrated circuit waveform generator which supplies a pulse train at a 14.7 kHz rate. The pulse train clocks a two stage counter as shown in Fig. 4. The first stage output is filtered to provide the 7.35 kHz reference sinusoid for the phase sensitive detector. The second counter stage synchronizes a free running magnetically coupled multivibrator the output of which is amplified in a switching amplifier to increase the power level for flux detector drive while preserving the original waveform symmetry.

Null Amplifier

Second harmonic voltages generated by the flux detector are converted to a dc current which flows through the 2,425 turn feedback winding to null the dc flux in the detector cores. This current also flows through a precision resistor bank to produce a voltage related to the primary bus current by:

$$E_0 = \frac{I_B R_L}{N_5}, \quad (3)$$

where I_B is the bus current, R_L is the metering resistor and N_5 is the number of turns of the feedback winding.

The second harmonic is extracted from the frequency spectrum generated by the flux detector with a commercial bandpass filter. The result is amplified and compared with the second harmonic reference sinusoid. A sinusoid, rather than a square wave is used as the reference to minimize the higher order harmonics in the output. The dc output of the phase comparator or multiplier is defined by

where K is an amplitude associated constant and ϕ is the phase difference. The multiplier gives a measure of the net dc flux seen by the detector cores in both sign and amplitude. This voltage is amplified in a frequency compensated high gain dc amplifier (A2 in Fig. 4).

In this transducer, the net dc flux must be kept to a minimum to prevent the decoupling core C_5 from saturating. Should this occur, excitation currents in the detector core assembly induce voltages in the feedback winding which in turn appear across the output metering resistor. To achieve the required measurement accuracy at 15 Hz, the low frequency response must be extended beyond 15 Hz. The measuring head has two important time constants to be considered. One is set by R_3 , the resistance of shorting turn N_3 and L_{C5} , the inductance of the feedback winding. A second is the L/R value of the feedback winding. The ultimate high frequency response (small signal) is the self-resonant frequency of the feedback winding.

Referring to Fig. 4, the $R_1 C_1$ product is selected to compensate for the frequency response of the feedback winding. Further improvement in frequency response can be carried out with a capacitor across R_5 (a lead network to offset the effect of the L_{C5}/R_3 time constant) or by bootstrapping with an additional winding (N_6).

A power output stage supplies the necessary ± 20 V at 500 mA to drive the feedback winding. The output voltage as determined by Eq. (3) requires a 20 Ω metering resistor for a 10 V output with a 1,212.5 A bus current. This rather significant impedance is buffered with a precision voltage follower which does not compromise the transducer's resolution.

To achieve a signal-to-noise ratio in excess of 100 dB, the measuring head signals are carefully isolated and shielded to minimize cross-talk and pickup. The dc null balance circuit is shielded to minimize pickup of noise generated by the ac excitation circuitry. These two circuits also have isolated grounding and power wiring.

A complete transducer system is shown in Fig. 5. It consists of two NIM modules, measuring head, and up to 10 m of cable enabling remote location of the measuring head. The transducer electronics is in a 2-wide NIM module, while the power supplies are in a 3-wide module. Two stages of magnetic shielding surround the measuring head to keep external fields below the point where they influence the operation of the transducer.

Conclusions

Second harmonic current transducers have been used on the Booster magnet power supply since it was commissioned. They have proven to be extremely repeatable and highly reliable devices.

Acknowledgments

The transducer testing and packaging was well performed by Marlon Palmer. One of us (ARD) wishes to thank his wife for her as usual last minute editing and typing assistance.

Reference

1. A. R. Donaldson and R. A. Winje, The NAL Booster Synchrotron Magnet Power Supply Servo, IEEE Transactions on Nuclear Science NS-20, 409 (1973).

Flux Detector Circuit

C_1, C_2, N_1
 C_3, C_4, N_4
 N_3

Null Balance Circuit

C_5, N_5, N_2

Fig. 1. Transducer measuring head with detail view of dc flux detector and feedback winding.

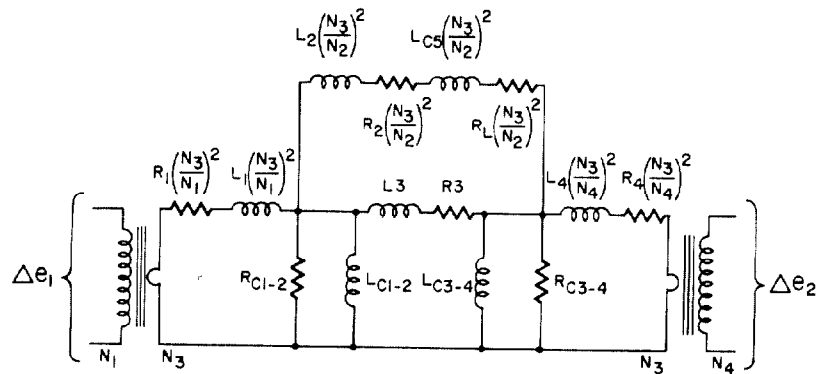
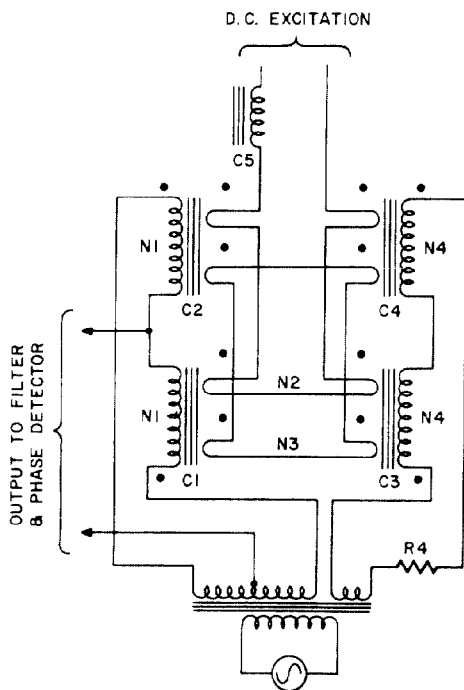
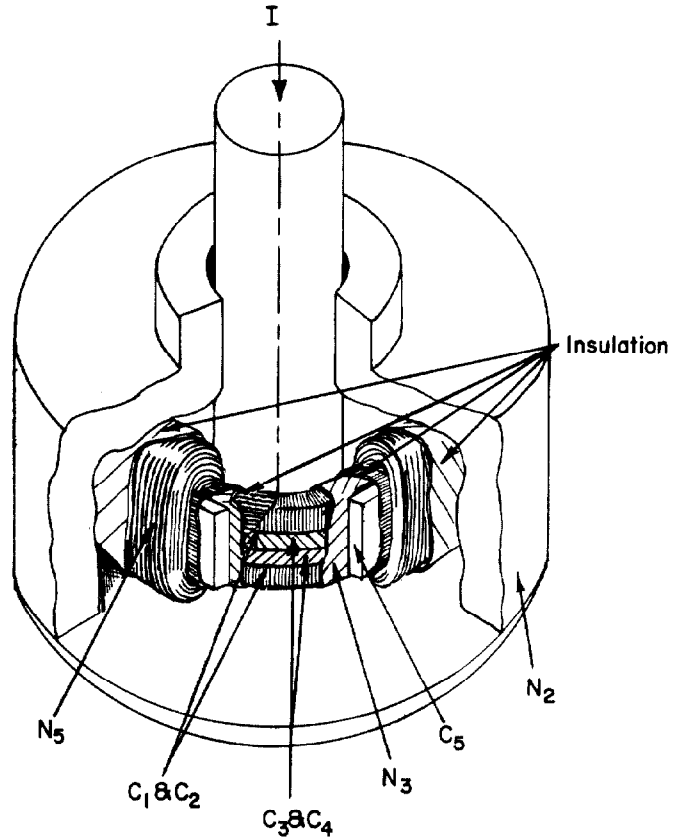


Fig. 2. Circuit configuration for dc flux measurement (a) and equivalent circuit (b).

Fig. 3. The measuring head and slotted current divider.

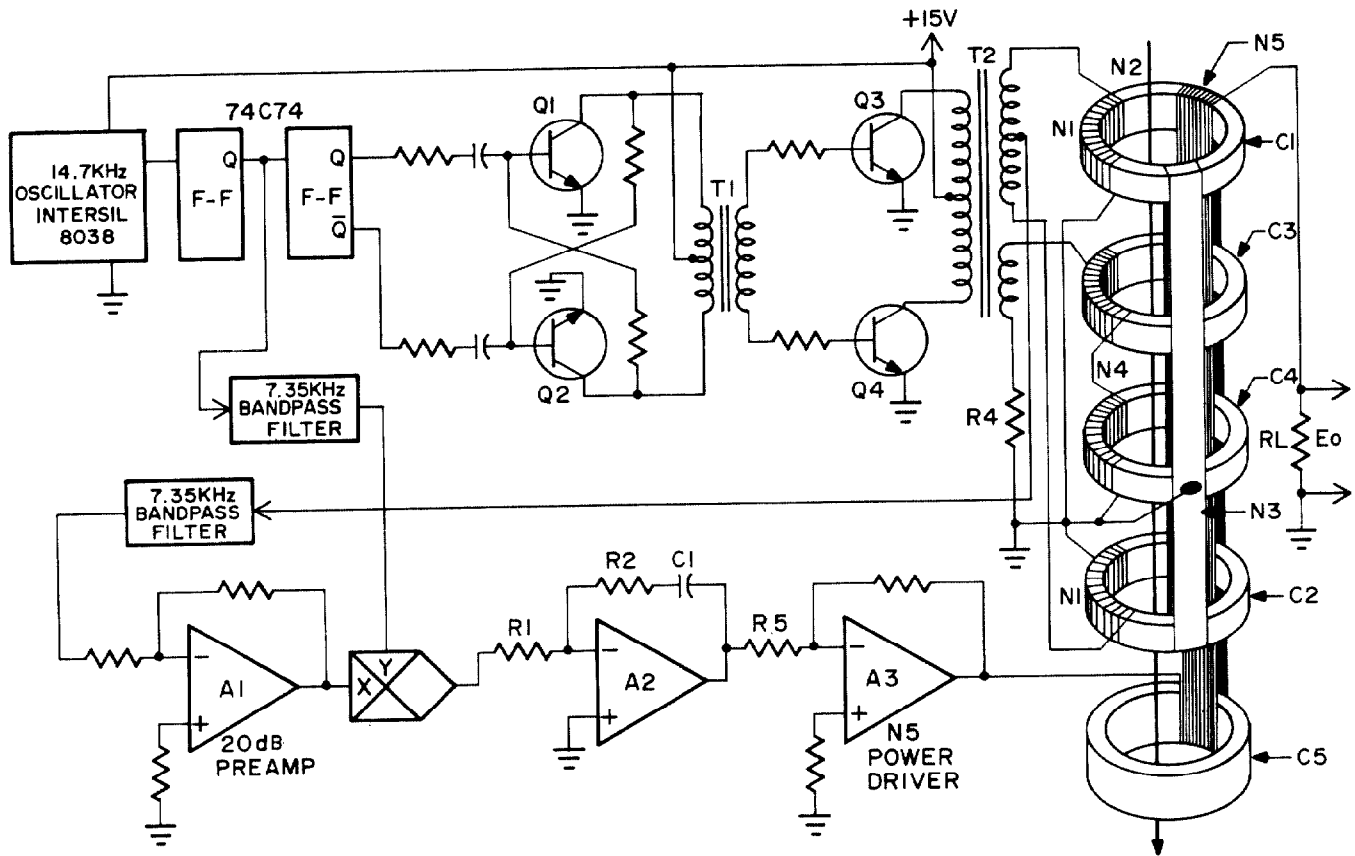
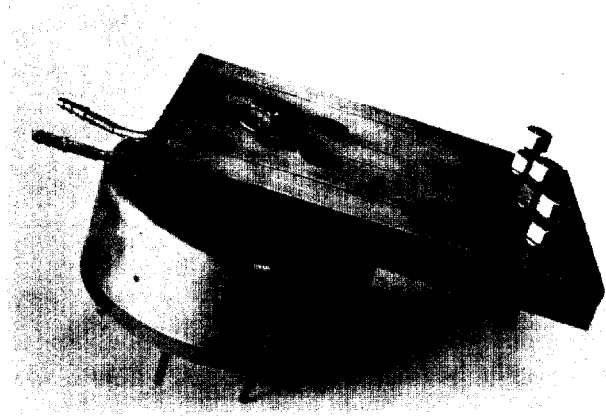


Fig. 4. Basic circuit of the transductor.

Fig. 5. The complete transductor system.

